MULTICOMPONENT ALLOY POWDERS PREPARATION BY MECHANICAL ALLOYING

MORAVČÍK Igor, ČÍŽEK Jan, DLOUHÝ Ivo

Institute of Materials Science and Engineering – NETME centre, Faculty of Mechanical Engineering, Brno University of Technology (BUT), Brno, Czech Republic

Abstract

In the last decade, multicomponent alloys arisen as new promising family of materials. The effect of milling parameters, namely milling balls size, milling speed and time on synthesis of inequiatomic AlCoCrFeNiTi0,5 mechanically alloyed (MA) powders in planetary ball mill were studied. Alloying behaviour, morphology, size and homogeneity of powders were observed by X-ray diffraction (XRD) and scanning electron microscopy (SEM). During MA, a supersaturated Cr based solid solution with BCC structure was formed after 24 hours of milling, with significantly reduced grain size. It was revealed, that selection of milling conditions have a great influence on milled powders properties. In general softer milling condition result in decreased particle size and homogeneity

Keywords: Multicomponent alloy, mechanical alloying, powder metallurgy, milling

1. INTRODUCTION

Multicomponent alloys (High-entropy alloys - HEA) proposed by Yeh et al. are alloys containing simple solid solutions consisting of more than four equimolar, or near equimolar elements. According to $\Delta G_{mix} = \Delta H_{mix} - T_m \Delta S_{mix}$ (equation for solid solutions where ΔG_{mix} is the Gibbs free energy, ΔH_{mix} is mixing enthalpy, T_m is melting temperature, and ΔS_{mix} is mixing entropy) high entropy of mixing derived from high configurational entropy stabilizes formation of simple disordered solid solution over intermediary phases [1]. Therefore these multicomponent alloys should have very simple structures instead of a mixture of ordered phases expected from Gibbs phase rule. Guo et al. investigated the relations between structures, valence electron concentrations (VEC), ΔH_{mix} , ΔS_{mix}, and δ (atomic size difference) as well as the electronegativity differences for formation of solid solutions, amorphous phases and intermetallic compounds. Formation of solid solution was found for $22 \leq \Delta H_{mix} \leq 7$ kJ/mol, $0 \leq \delta \leq 8.5\%$, and $11 \leq \Delta S_{mix} \leq 19.5$ J/(K.mol) [2, 3]. This concept is different from conventional strategy for developing metallurgical alloys where the main component based on a primary property requirement is selected, and use of alloying additions to improve secondary properties is employed. This strategy has led to many multicomponent alloys based on a single main component [4]. In the case of multicomponent alloys it is impossible to distinguish main component. This approach significantly expands the potential for designing new alloy compositions.

In theory, multicomponent alloys should benefit from solid solution strengthening derived from many elements with different atomic radii present in the lattice, causing severe lattice strain, while retaining reasonable ductility resulting from many slip systems of disordered face centered cubic (FCC) or body centered cubic (BCC) structure. [5]. Recently, Tsai [6] measured diffusion coefficients in single phase HEA, and compared the diffusion coefficients for the elements in pure metals and stainless steels. He has found that the order of diffusion rates is slowest in HEA. The sluggish diffusion effect is usually used to explain the formation of nano-sized precipitations, due to their slow growth [7]. This phenomenon could lead to interesting high temperature properties due to increased phase stability observed by Senkov [8]. The effect of addition of the Al content in various HEAs based on CoFeNiAl on their structures, thermodynamics, and mechanical properties has been reviewed and analysed by Tang [9]. Apparently introduction of element with bigger atomic radii (Al,Ti) stabilizes formation of BCC phase.

Previous studies showed that the AlCoCrFeNiTi_x alloy system (x = 0, 0.5, 1.0, and 1.5 in molar ratio) has promising mechanical properties. Especialy $\text{AlCoCrFeNiTi}_{0.5}$ has a yield strength, fracture strength, and plastic strain limit 2.26 GPa, 3.14 GPa, and 23.3%, respectively [10]. Another interesting aspect of this alloy is its low density 6.67g/cm^3, by 14,5% lower than for high strength steels.

In the most cases, HEAs are produced by standard metallurgy approach – casting. However many issues can be associated with this process like interdendritic segregations, evaporation of lower melting elements etc. Preparation of HEA by powder metallurgy (PM) route could lead to many benefits derived from avoiding liquid phase formation. Process most suitable for production of HEA is mechanical alloying [11]. Mechanical alloying (MA) is a solid-state powder-processing technique involving repeated cold welding, fracturing, and re-welding of powder particles in a high-energy mill [12]. MA has now been shown to be capable of synthesizing a variety of equilibrium and non-equilibrium alloys including amorphous and nanostructured materials from elemental powders [7, 12]. However in the MA process, the end result of the milling even for one alloy composition is greatly altered by milling parameters (milling time, milling speed, ball to powder ration, milling medium size, PCA etc.) [13-15]. Solid solution, intermediate or amorphous phase can form in the same alloy, with different morphology and particle size distribution [13-15]. To the author's best knowledge, there has been no reports on preparation of $\text{AlCoCrFeNiTi}_{0,5}$ by powder metallurgy and detailed study on milling parameters on any HEA has also not been carried out yet. Consequently $\text{AlCoCrFeNiTi}_{0,5}$ powders have been synthetized by MA with respect to milling parameters influence.

2.EXPERIMENTAL

The powders with nominal composition of $\text{AlCoCrFeNiTi}_{0.5}$ (in atomic proportion) were prepared by milling of mixed elemental powders. Elemental powders Fe, Ni, Cr, Al, Co and Ti with high purity and particle size of around 45 µm (325 mesh) were placed in high performance hardened steel milling bowl and sealed together with milling medium (hardened steel balls) under Ar atmosphere. Small amount of methanol was used as a process control agent. Constant 1:10 ball to powder weight ratio (BPR) was used for all milling. The sealed vial was then fitted in a high energy planetary ball milling machine (Pulverisette 6). Different milling parameters (ball size, RPM and time) were used to investigate their influence on end product, see table1. Milling was regularly stopped to prevent overheating of the bowl for same time periods and pauses time. Produced powders were evaluated using Carl Zeiss Ultra scanning electron microscope (SEM) and Phillips X-ray diffractometer (XRD) with a Cu Kα radiation XRD analysis for phase composition, elements distribution and particle and grain size.

2.1 Milling energy calculation

The energy input during ball milling is calculated using the standard formulation in [15] The velocity of the ball (V_b) is given by the following expression:

$$V_b = \frac{2\pi}{60}\left[Rp^2\Omega^2 + (R_v - R_b)\omega^2\left(1 + 2\frac{\omega}{\Omega}\right)\right]^{0.5} \qquad (1)$$

Here R_p, R_v and r_b are the radii of the plate, vial and the balls, respectively, ω and Ω are the angular velocity of the vial and the plate. The kinetic energy of the one ball E_b is given by equation:

$$E_b = 0.5 m_b v_b^2 \qquad (2)$$

with m_b being weight of one ball. Total milling intensity I_t (energy per weight unit of powder) is given by:

$$I_t = \frac{\emptyset E_b N_b t}{W_p} \qquad (3)$$

where N_b is the number of balls, t is milling time, W_p is weight of milled powder and $\varnothing$ filling factor of the vial taking into account efficiency of milling (0.95 in case of one third of the vial filled). The milling process can be altered by many other parameters, either way it is sufficiently described by these equations for previous research trials.

Table 1 milling conditions and calculated parameters

Milling number	RPM	BPR	Time(h)	Ball D (mm)	PCA	Mil. Intensity I_t (J/g)
1	250	1:10	10	10	Methanol	834
2	250	1:10	24	10	Methanol	2002
3	250	1:10	10	15	Methanol	784
4	250	1:10	24	15	Methanol	1883
5	400	1:10	10	10	Methanol	2135
6	400	1:10	24	10	Methanol	5125
7	400	1:10	10	15	Methanol	2009
8	400	1:10	24	15	Methanol	4822

3. RESULTS AND DISCUSSION

Figure 1 and 2 show XRD patterns of mechanically alloyed powders with different milling times, RPM and ball diameters. Sharp peaks of respective elements are observed in initial state (0h). After 10 hours of milling with 250 RPM, peaks start to join together and their intensity decreases. This process can be considered as a start of solid solution forming reaction. In generally higher bonding energy between atoms is expressed by increase in melting temperature and decrease in diffusion coefficient. Our observation is in accordance with this consideration. Elements with lower melting points, especially aluminium start to dissolve in lattices of elements with higher melting points like iron and chromium. In the end, all elemental peaks disappear and only one body centered cubic (BCC) solid solution forms with peaks in original chromium and iron peaks places with almost perfect $AlCoCrFeNiTi_{0,5}$. This phenomenon is often associated also with atomic packing factor of BCC lattice, which is considerably lower, compared to FCC lattice. Because of this, BCC solid solution can accommodate more atoms with different radii and solubility is higher. Fu et. al [11] prepared alloyed powders with very close composition of $Al_{0.5}CoCrFeNiTi_{0,5}$ and they reported formation of mixture of FCC and BCC solid solutions after 42 hours of milling. It seems addition of Aluminium promotes formation of BCC solid solution over FCC. This result is in agreement with work of Wang et al. [16].

When we look at the differences between the usages of 10 or 15 millimetre balls, for all cases the XRD patterns look very similar. Only minor changes in peak intensities could be observed. This phenomenon can be associated with differences in milling intensity (table 1). It seems that the usage of 10mm balls can induce slight increase in milling intensity for all milling cases. Even thou one 15 mm ball have higher weight and subsequently kinetic energy, for same BPR, much more 10 mm balls must be used. In the end, total kinetic energy of 10 mm balls together is moderately higher, therefore also intensity for same time is higher. As expected, comparison between 250 and 400 RPM of milling speeds revealed that higher milling speed causes improvement in milling intensity and faster alloying. Very interesting is the fact that even if calculated milling intensities for 10 hours with 400 RPM and 24 hours with 250 RPM are very close (especially for milling number 2 and 7), XRD patterns are very different, with much broader peaks suggesting comparably smaller crystallite sizes and overall much better alloying in case of 400 RPM use. One possible explanation of this effect can be significant increase of milling bowl temperature during milling with higher RPM. To prevent bowl from overheating, milling was stopped to allow cooling of the mill and bowl, but to preserve similar conditions for all cases, same cooling times and intervals were used. This on the other hand resulted in increased temperature rising for higher RPM. It was not possible to record milling bowl temperature rise directly, although cooling times were selected so that temperature never exceeded 70 C˚ on the surface of the bowl measured after end of milling. It is questionable if temperature inside milling bowl could have reached higher values, leading to some considerable effects on powder plasticity, diffusion kinetics etc. resulting in different alloying behaviour. Further investigation in this area is needed. Nevertheless in general efficiency of milling is greatly improved if higher RPM is used.

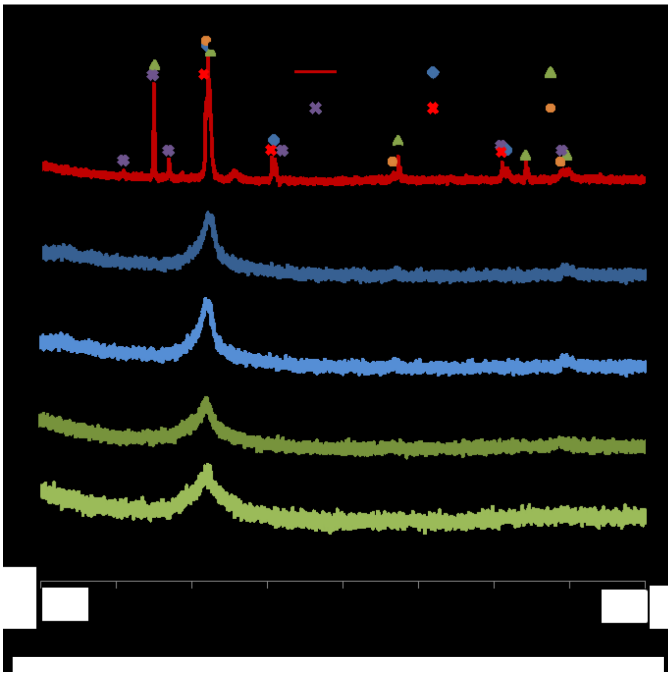

Fig. 1 XRD results of $AlCoCrFeNiTi_{0,5}$ powders after different milling times and balls diameters at 400 RPM

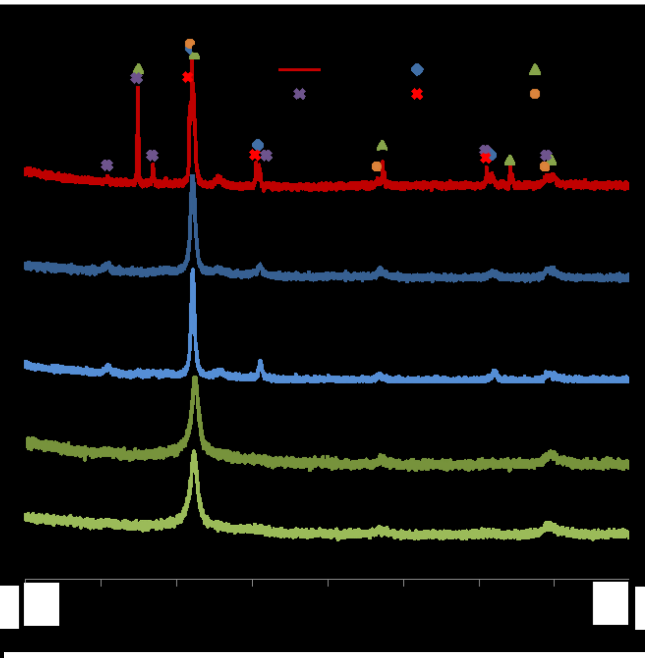

Fig. 2 XRD results of $AlCoCrFeNiTi_{0,5}$ powders after different milling times and balls diameters at 250 RPM

SEM images of the $AlCoCrFeNiTi_{0,5}$ high-entropy alloy powders under different milling conditions with utilization of 15mm balls are shown in Figure 3 and 4. For elements homogeneity representation, only chromium and iron maps are needed. These elements are hardest do disperse and if these are evenly distributed, the other elements are dispersed as well. During mechanical alloying the powders are crushed between milling media and bowl resulting in flake like morphology after 10 hours with speed of 250 RPM. This is defined as the first stage of alloying for ductile materials. As seen from EDS maps of this powder the homogeneity is very poor and individual particles of original elements are present. With increasing intensity of milling (either by increasing speed or time) intensive fracturing and re-welding of particles take place. This improves the homogeneity and changes the particle morphology. As we can see the milling conditions greatly influence especially the particle size. Comparison between 250 and 400 RPM milling speed shows much coarser particle size in case of using 400 RPM for all instances but on the other hand almost perfect homogeneity even after only 10 hours of milling with even distribution of all elements according to EDS maps. Further milling with 400 RPM only increases particle size as seen in Fig. 3a. In cases of using 250 RPM speed, distribution of hardest elements is imperfect even after 24 hours of processing. This shows much better process efficiency for higher milling speeds and is in accordance with previous result from XRD. The complementary experiementswith 10 mm balls generally have shown small differences in particle sizes and less homogenous element distribution. This could be explained by lower kinetic energy of smaller balls being somewhat insufficient to fracture harder elemental particles.

CONCLUSIONS

Multicomponent alloy powders of $AlCoCrFeNiTi_{0,5}$ were successfully synthetized by mechanical alloying process. From previous results we can conclude, that selection of process parameters is very important factor for achieving good end product properties and process efficiency. By adjustment of process variables,

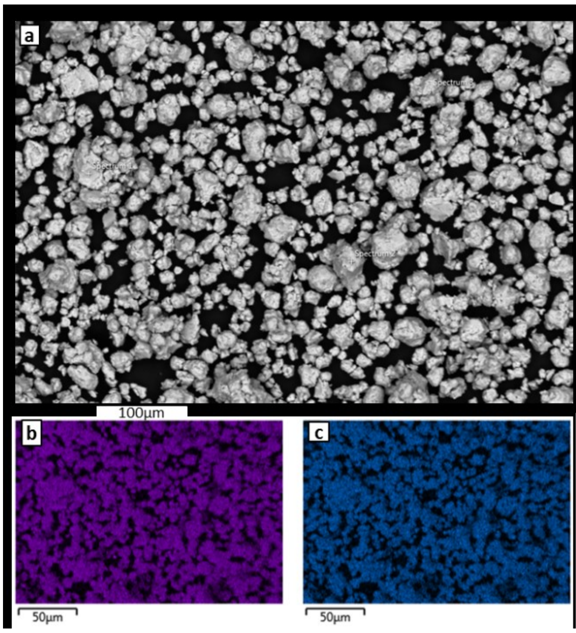

Fig. 3 a) SEM images of powder for 10 hrs of 400 RPM milling,15 mm balls b) Cr map c)Fe map

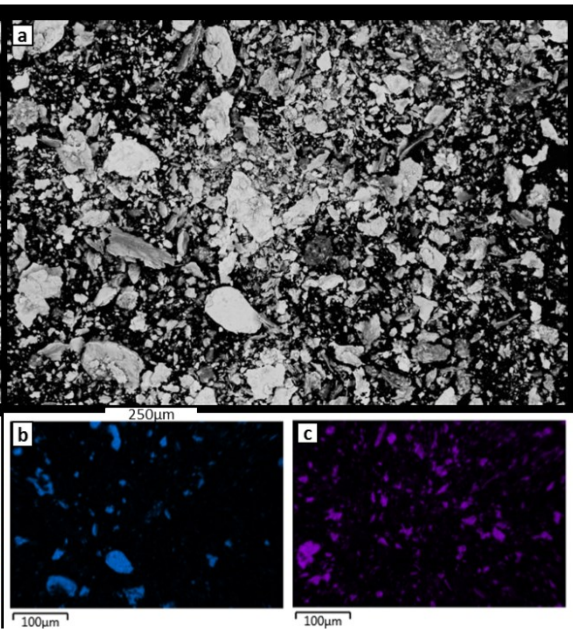

Fig. 3 b) SEM images of powder for 10 hrs of 250 RPM milling,15 mm balls b) Cr map c)Fe map

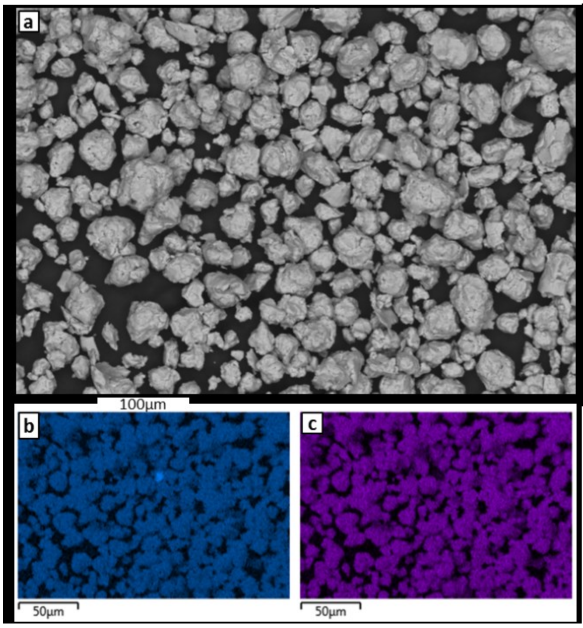

Fig. 4 a) SEM images of powder for 24 hrs of 400 RPM milling,15 mm balls b) Cr map c)Fe map

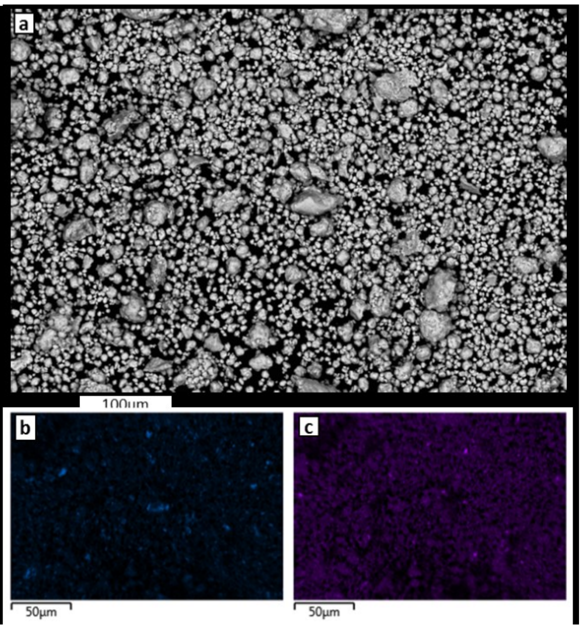

Fig. 4 b) SEM images of powder for 24 hrs of 250 RPM milling,15 mm balls b) Cr map c)Fe map

it is possible to obtain different results depending on desired properties, which can be different for different following sintering procedures. For presureless sintering, best densification is obtained when particle size is as small as possible for needs of best die filling. For pressure assisted processes like spark plasma sintering, highest homogeneity is desirable bearing in terms of very short sintering times (limited diffusion). If we consider combination of the best homogeneity, crystallite grain refinement and smallest particle size (for improved densification), 10 hours of mechanical alloying with 15 mm balls and 400 RPM milling speed should be used, with utilization of 10:1 BPR and methanol as process control agent. In general, use of higher speeds which greatly improves process efficiency, even for the same intensities, by using bigger milling ballsis suggested.

ACKNOWLEDGEMENTS

The research was co-funded by the Ministry of Education, Youth and Sports within the „National Sustainability Programme I" (NETME CENTRE PLUS - LO1202). Support to Czech Science Foundation project GACR 13-35890S is further acknowledged

REFERENCES

[1] J. W. Yeh, S. K. Chen, S. J. Lin, J. Y. Gan, T. S. Chin, T. T. Shun*, et al.*, "Nanostructured High-Entropy Alloys with Multiple Principal Elements: Novel Alloy Design Concepts and Outcomes," *Advanced Engineering Materials,* vol. 6, pp. 299-303, 2004.

[2] S. Guo and C. T. Liu, "Phase stability in high entropy alloys: Formation of solid-solution phase or amorphous phase," *Progress in Natural Science: Materials International,* vol. 21, pp. 433-446, 12// 2011.

[3] S. Guo, Q. Hu, C. Ng, and C. T. Liu, "More than entropy in high-entropy alloys: Forming solid solutions or amorphous phase," *Intermetallics,* vol. 41, pp. 96-103, 10// 2013.

[4] B. Cantor, I. T. H. Chang, P. Knight, and A. J. B. Vincent, "Microstructural development in equiatomic multicomponent alloys," *Materials Science and Engineering: A,* vol. 375–377, pp. 213-218, 7// 2004.

[5] Y. Zhang, T. T. Zuo, Z. Tang, M. C. Gao, K. A. Dahmen, P. K. Liaw*, et al.*, "Microstructures and properties of high-entropy alloys," *Progress in Materials Science,* vol. 61, pp. 1-93, 4// 2014.

[6] K. Y. Tsai, M. H. Tsai, and J. W. Yeh, "Sluggish diffusion in Co–Cr–Fe–Mn–Ni high-entropy alloys," *Acta Materialia,* vol. 61, pp. 4887-4897, 8// 2013.

[7] C. S. Babu, N. T. B. N. Koundinya, K. Sivaprasad, and J. A. Szpunar, "Thermal Analysis and Nanoindentaion Studies on Nanocrystalline AlCrNiFeZn High Entropy Alloy," *Procedia Materials Science,* vol. 6, pp. 641-647, // 2014.

[8] O. N. Senkov, G. B. Wilks, J. M. Scott, and D. B. Miracle, "Mechanical properties of Nb25Mo25Ta25W25 and V20Nb20Mo20Ta20W20 refractory high entropy alloys," *Intermetallics,* vol. 19, pp. 698-706, 5// 2011.

[9] Z. Tang, M. Gao, H. Diao, T. Yang, J. Liu, T. Zuo*, et al.*, "Aluminum Alloying Effects on Lattice Types, Microstructures, and Mechanical Behavior of High-Entropy Alloys Systems," *JOM,* vol. 65, pp. 1848-1858, 2013/12/01 2013.

[10] Y. Wang, S. Ma, X. Chen, J. Shi, Y. Zhang, and J. Qiao, "Optimizing mechanical properties of AlCoCrFeNiTi x high-entropy alloys by tailoring microstructures," *Acta Metallurgica Sinica (English Letters),* vol. 26, pp. 277-284, 2013/06/01 2013.

[11] Z. Fu, W. Chen, S. Fang, and X. Li, "Effect of Cr addition on the alloying behavior, microstructure and mechanical properties of twinned CoFeNiAl0.5Ti0.5 alloy," *Materials Science and Engineering: A,* vol. 597, pp. 204-211, 3/12/ 2014.

[12] C. Suryanarayana, "Mechanical alloying and milling," *Progress in Materials Science,* vol. 46, pp. 1-184, 1// 2001.

[13] J. Joardar, S. K. Pabi, and B. S. Murty, "Milling criteria for the synthesis of nanocrystalline NiAl by mechanical alloying," *Journal of Alloys and Compounds,* vol. 429, pp. 204-210, 2/21/ 2007.

[14] N. C. Abhik, R. Vivek, V. Udhayabanu, and B. S. Murty, "Influence of heat of formation of B2/L12 intermetallic compounds on the milling energy for their formation during mechanical alloying," *Journal of Alloys and Compounds,* vol. 465, pp. 106-112, 10/6/ 2008.

[15] B. S. Murty, M. Mohan Rao, and S. Ranganathan, "Milling maps and amorphization during mechanical alloying," *Acta Metallurgica et Materialia,* vol. 43, pp. 2443-2450, 6// 1995.

[16] W.-R. Wang, W.-L. Wang, S.-C. Wang, Y.-C. Tsai, C.-H. Lai, and J.-W. Yeh, "Effects of Al addition on the microstructure and mechanical property of AlxCoCrFeNi high-entropy alloys," *Intermetallics,* vol. 26, pp. 44-51, 7// 2012.